

Design of the 48, 57 μm Poloidal Polarimeter for ITER

Rostyslav PAVLICHENKO, Kazuo KAWAHATA and Tony DONNÉ¹⁾

National Institute for Fusion Science, Toki 509-5292, Japan

¹⁾FOM-Institute for Plasma Physics Rijnhuizen, Nieuwegein NL-3439, Netherlands

(Received 5 December 2006 / Accepted 13 May 2007)

Polarimetry diagnostic for International Thermonuclear Experimental Reactor (ITER) considered among the tools to measure and, thus, to provide ability to control the thermonuclear plasma in the next generation fusion device. The shortage of the reliable sources in the short wavelength far infrared (FIR) region suggests to use common CH_3OH oscillation line. Recently new laser sources became available at $50\mu\text{m}$ FIR region. Proposed system unveil the alternative possibilities apart from $118.8\mu\text{m}$ poloidal polarimeter for ITER. This system, which introduces 47.6 and $57.2\mu\text{m}$ oscillation lines of CO_2 -laser pumped CH_3OD laser inherits all well documented features from it $118.8\mu\text{m}$ predecessor will shows the clear advantages to utilize shorter wavelength radiation for plasma probing.

© 2007 The Japan Society of Plasma Science and Nuclear Fusion Research

Keywords: polarimetry, plasma fusion diagnostics, ITER

DOI: 10.1585/pfr.2.S1040

1. Introduction

Control of the current density profile (the safety factor profile can provide very effective internal constraints for the reconstruction of magnetic equilibria) becomes a paramount issue for the future tokamak experiments. Polarimetry (an instrument for measuring the polarization of light, and for determining the effect of a plasma in rotating the plane of polarization of light) can provide information on the density and magnetic field from which current profile could be reconstructed.

2. Basic Layout of the Polarimeter

The polarimeter system that presented here is evolved from the previous designs: ITER-98 and ITER-FEAT [1,2]. Previous system was design to operate at $\lambda = 118.8\mu\text{m}$ CH_3OH oscillation line. It is well known that there are two main approaches to build the polarimetry system. To obtained information about magnetic field one have to measure the value of Faraday rotation angle α_F , which is proportional to poloidal magnetic field (its component parallel to the beam line) $B_{p\parallel}$ and electron density n_e .

$$\varphi_{\text{INT}} = 2.82 \times 10^{-15} \lambda \int_Z n_e(z) dz. \quad (1)$$

$$\alpha_F = 2.62 \times 10^{-13} \lambda^2 \int_Z n_e(z) B_{p\parallel}(z) dz. \quad (2)$$

From α_F values profile of the poloidal component of the magnetic field could be calculated. It became obvious that the quantity of the electron density along very same beam line have to be known. For this purpose along beam chord

author's e-mail: pavlichenko.rostyslav@LHD.nifs.ac.jp

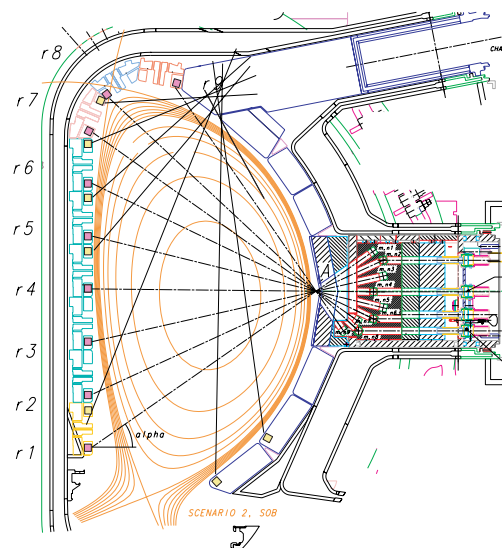


Fig. 1 ITER cross-section with horizontal 'beam-fan' lines from the first plane mirror to retroreflector. Additional vertical chords, which are inserted from upper port plug are shown only for reference.

an interferometric measurements φ_{INT} or measurements of the ellipticity angle α_{CM} (Cotton-Mouton effect or plasma birefringence) have to be performed.

$$\alpha_{\text{CM}} = 2.45 \times 10^{-11} \lambda^3 \int_Z n_e(z) B_t^2(z) dz. \quad (3)$$

maximum number of twelve probing beams comes into the plasma through the diagnostic plug at the low-field side (LFS). All chords have the same single crossing point at the edge of the blanket shield module (BSM)

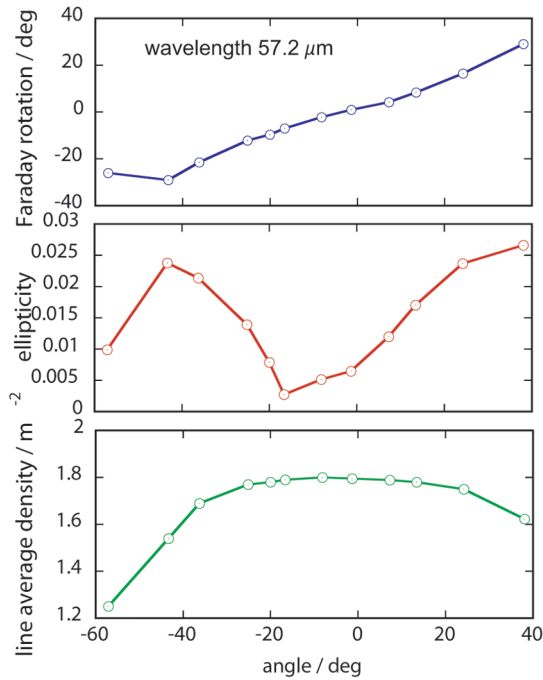


Fig. 2 Calculated Faraday (top) rotation and ellipticity (middle) and averaged line density (bottom) for wavelength 57 μm for the single passage through the plasma.

(see Fig. 1). They almost quasi-equidistantly cover entire poloidal plasma section. The orientation of the chords is that there is no toroidal component of the magnetic field along the line of sight. At the high-field side (HFS) of the BSM small ($\varnothing 37$ mm) corner retroreflectors (CRR) are placed to reflect backwards the laser beams.

Recently for ITER-scale experiments and for the plasma experiments on Large Helical Device (LHD) we have been developing short wavelength FIR laser. This research activities are carried out to overcome the common ‘fringe jumps’ phenomena which occurs because of electron density increasing during pellet injection experiments. On LHD 13-channel $119\ \mu\text{m}$ CH_3OH laser interferometer has routinely operated to provide information on the electron density profile. The wavelengths of the new two-color interferometer are $57.2\ \mu\text{m}$ (~ 1.6 W) and $47.6\ \mu\text{m}$ (~ 0.8 W) in a twin optically pumped CH_3OD laser [3, 4]. Since $47.6\ \mu\text{m}$ and $57.2\ \mu\text{m}$

For ITER experiments we advocate the classical interferometer / polarimeter approach for its considerable simplicity to reconstruct experimental data. We consider the propagation of polarimeter beams through a thin (layer of plasma thickness z_0) in the presence of a magnetic field. The Jones matrix, \mathbf{S} , for the homogeneous layer of the plasma through which laser beam is penetrate, takes place in z -direction and where the magnetic field is taken to be in the $y - z$ plane is [6].

$$\mathbf{S} = \begin{pmatrix} S_{11} & S_{12} \\ S_{21} & S_{22} \end{pmatrix} \quad (4)$$

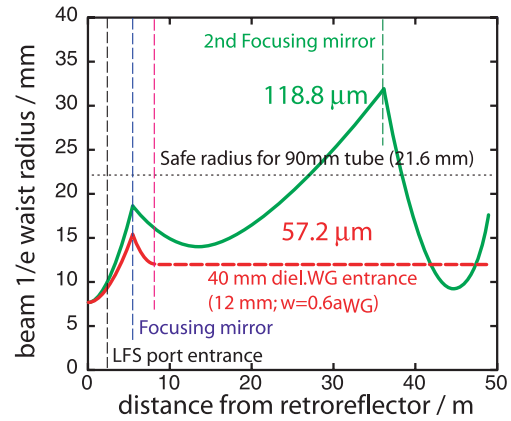


Fig. 3 Calculated Gaussian beam radius (waist of 1/e intensity value) for wavelength 118 and 57 μm ; position of the several optical elements are shown as dotted lines.

where, $S_{11} = \cos \frac{\varphi}{2} + i \frac{1-a^2}{1+a^2} \sin \frac{\varphi}{2}$, $S_{12} = \frac{2\alpha}{1+a^2} \sin \frac{\varphi}{2}$, $S_{21} = \frac{-2\alpha}{1+a^2} \sin \frac{\varphi}{2}$, $S_{22} = \cos \frac{\varphi}{2} - i \frac{1-a^2}{1+a^2} \sin \frac{\varphi}{2}$, the polarization coefficient, α , is

$$\alpha = \frac{Y \sin^2 \theta}{2(1-X) \cos \theta} - \sqrt{1 + \left(\frac{Y \sin^2 \varphi}{2(1-X) \cos \varphi} \right)^2} \quad (5)$$

where, $X = \omega_p^2 / \omega^2$ and $Y = \omega_c / \omega$, angle θ - is the angle between the direction of propagation and magnetic field B_0 . The parameter φ represents the phase shift in the characteristic propagating modes:

$$\varphi = \frac{\omega}{c} (\mu_- - \mu_+) \quad (6)$$

the quantities μ_- and μ_+ are the refractive indices of the two characteristic modes, which are given by Appleton-Hartree formula. The Jones matrix takes into account both the Faraday rotation and the Cotton-Mouton effect.

The calculation of the expected values of Faraday rotation angle and ellipticity for chosen ITER ‘plasma burn’ scenario (plasma current $I_p = 15.0197$ MA, $q_0 = 0.99$, ‘flat’ electron density profile (as a function of normalized poloidal flux function Ψ_{norm}) of form: $n_e(\Psi_{norm}) = (n_e(0) - 10^{19} \text{ m}^{-3}) \{1 - (\Psi_{norm})^8\}^2 + 10^{19} \text{ m}^{-3}$, with ‘central’ density $n_e(0) = 2.0 \times 10^{20} \text{ m}^{-3}$ and plasma pressure profile of form $P(\Psi_{norm}) [\text{MA}] = 0.8 \times \{1 - (\Psi_{norm})^2\}^2$) are shown at the Fig. 2. One can see that for the chosen wavelength of $57.2\ \mu\text{m}$ Faraday rotation angle is about $25 - 30^\circ$, which is still large enough to perform accurate measurements (even in the case when polarimeter have a modest accuracy $\approx 1.5\text{-}2.0^\circ/\text{m}$).

3. Two Color Interferometer

Recently for ITER-scale experiments and for the plasma experiments on Large Helical Device (LHD) we have been developing short wavelength FIR laser. This research activities are carried out to overcome the common

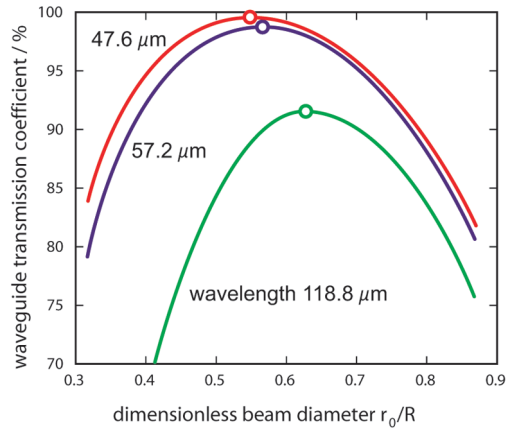


Fig. 4 Optimization of the laser beam diameter for coupling of Gaussian beam at the entrance plane of the dielectric waveguide, for wavelength of 47.6 μm , 57.2 μm and 118.8 μm .

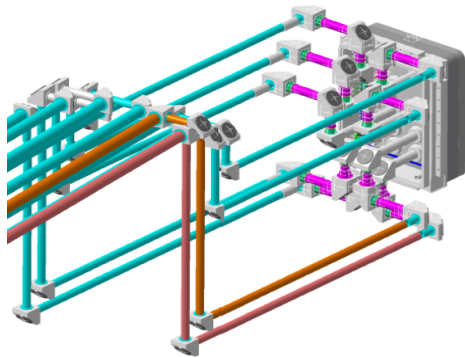


Fig. 5 Poloidal polarimetry transmission lines and port plug to tokamak.

‘fringe jumps’ phenomena because of rapid raise of the plasma electron density, which occurs during pellet injection experiments. On LHD 13-channel 118.8 μm CH_3OH laser interferometer has routinely operated to provide information on the electron density profile. The wavelengths of the new two-color interferometer are 57.2 μm (power 1.6 W) and 47.6 μm (power 0.8 W) in a twin optically pumped CH_3OD laser [2, 3]. Since 47.6 μm and 57.2 μm have different polarization a Martin-Puplett diplexer is placed in front of the laser output. One of the most important issue is the developing of high quality heterodyne detection system with fast and sensitive characteristics. After investigating among several candidates we finally chose a gallium-doped germanium detector operating at liquid He temperature.

4. Transmission Line and Corner Retroreflectors

One of the main differences from 118.8 μm system is that instead of using quasi-optical transmission line (evacuated tubes of 90-120 mm in diameter) 40 mm dielectric

waveguides (made from Pyrex[®] borosilicate glass (with relative dielectric constant $\epsilon_r = 4.6\text{-}5.0$) or acrylic resin ($\epsilon_r = 2.7\text{-}6.0$)) become an attractive candidate.

Determination of life-time for glass/dielectric components becomes high priority research task. Oversized waveguides offer an attractive practical solution to transport light through the complicated geometry surrounding the fusion reactor. However, they can suffer from serious radiation-induced optical absorption and radio-luminescence. Special fabrication and glass hardening techniques must be developed before suitable radiation-resistance dielectric waveguides can be used in ITER [11, 12].

By switching from pure quasi-optical (QO) beam free space propagation to ‘miter bend + oversized waveguide ideology’ for the transmission line that lies outside port plug (transmission line that correspond to the straight line at the Fig. 3) we can resolve several obstacles such as: mode matching/mode conversion, misalignment in the ‘middle part’ of the polarimeter optical path, which will be very difficult to maintain. From other hand waveguide system has precise mode matching (see Figs. 3, 4) (defined by waveguide diameter), easy alignment and more robust to mechanical vibrations. To deliver radiation from/to plasma each laser beam line is equipped with up to 8 miter-bends, Fig. 5. The conversion losses (CL) per unit are:

$$\text{CL} = \left(\frac{\lambda}{c}\right)^{1.5} = 3.83 \times 10^{-5}, \text{ dB} \quad (7)$$

To avoid beam power dissipation Gaussian beam must enter the waveguide having optimized diameter. The calculation of waveguide transmission coefficient (according to [8]) have been done for 48, 57, 118.8 μm

$$T = \left(1 - \exp\left(-F \frac{R^2}{r_0^2}\right)\right) F^{-1} \quad (8)$$

where $F = 1 + \frac{\epsilon_r + 1}{\sqrt{\epsilon_r - 1}} \frac{L}{R} \frac{1}{k^2 r_0^2}$ and R , L -waveguide radius and length, $k = 2\pi/\lambda$ -laser beam wavelength, r_0 -radius of the $1/e$ beam intensity level at the waveguide entrance, waveguide material (relative dielectric constant) was chosen such as: $\sqrt{\epsilon_r} = 2.1$. The calculation (refer to Fig. 4) shows that transmission coefficient values for 47.6 and 57.2 coupling into 40 mm diameter waveguide are about 99.6-98.42%, which is 7-8% higher than that for 118.8 μm . From this calculation we can conclude that from the transmission coefficient at least, that beam propagation inside the oversized dielectric waveguide have the same efficiency as for the free space propagation, thus, preserves its polarization (99.6%). It was already confirmed by the long-term operation of FIR interferometer at LHD [7] (acrylic resin waveguide, length about 40 m) and from several reports on JET [10] polarimeter diagnostic (pyrex glass waveguide, length about 30 m) that polarization of the laser beam in the waveguide remains almost constant.

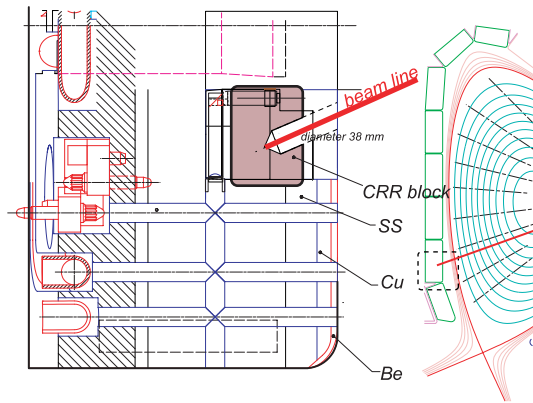


Fig. 6 General view of the polarimetry retroreflectors mounted in blanket RH gripper holes.

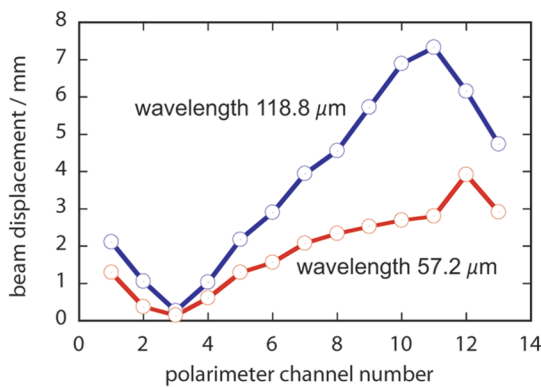


Fig. 7 Beam displacement characteristics at corner retroreflectors as a function of laser beam channel number.

It was already shown [2, 5] by other research groups mechanical and optical properties of the corner retroreflectors became ultimately ‘Achilles heel’ of the system. The positions of the retroreflectors are limited by mechanical design of blanket shield modules on HFS inner wall. It was found that for wavelength 118.8 μm previously, that CRR can cope with misalignment up to 15-20 mm in poloidal plane without any serious effect on the reflectivity. For the shorter wavelength those values become twice smaller: up to 7.5 mm (see Fig. 7). This gives us much more freedom to cope with beam displacement caused by mechanical vibrations and due to refraction in plasma. Present level of CRR manufacturing could deal with ‘ideal’ sharp corner to sustain desirable sharpness which is about 5 % from the laser beam width.

5. Summary

Recently proposed poloidal high power polarimeter will operate at 47.6 μm, 57.2 μm infrared oscillation. The output power of 57.2 μm laser is estimated to be over 1.6 W and that of 47.6 μm is about 0.8 W. Two color beat signals are simultaneously detected by a Ge:Ga detector with success. It was shown that preferable polarimeter-

interferometer configuration will unveil some extra advantages in respect of ‘full-polarimetric’ system. Over years polarimetry - interferometry was well established techniques, a lot of experience and scientific data on this subject. Shorter wavelength laser will significantly improve (diminish) refraction problems. For present chord alignments and beam wavelength caused considerably small Cotton-Mouton effect. Alternated waveguide transmission line (with miter bends included) showed better focusing and tuning as well as much simple further maintenance. High power two color beat signals are simultaneously detected by a Ge:Ga detector; it is possible to suppress fringe jumps and mechanical vibrations. One must say that real advantage of the Cotton-Mouton polarimeter becomes clear only in the case when the viewing chords are orientated in the equatorial plane, where the poloidal component of the magnetic field B_p is zero (pure toroidal polarimetry). There are several problems that we have to address. Under some plasma condition there is a possibility of coupling Faraday and Cotton-Mouton effects. Small Faraday rotation angle along some central chords suggests that placing additional beam lines must be done to improve spatial resolution of the system.

Promotion of the dielectric waveguide addresses the issue of the radiation effect on those components. The appropriate additional ‘shielding’ of the waveguides now under the consideration. Further research are needed to define the most adapted materials for dielectric waveguides for FIR polarimetry [12].

- [1] A.J.H. Donn , M.F. Graswinckel, M. Cavinato, L. Giudicotti, E. Zilli, C. Gil, H.R. Koslowski, P. McCarthy, C. Nynhan, S. Prunty, M. Spillane and C. Walker, *Rev. Sci. Instrum.* **70**, 726 (1999).
- [2] A.J.H. Donn , T. Edlington, E. Joffrin, H.R. Koslowski, C. Nieswand, S.E. Segre, P.E. Stott and C. Walker, *Rev. Sci. Instrum.* **75**, 4701 (2004).
- [3] K. Kawahata, K. Tanaka, T. Tokuzawa, T. Akiyama, Y. Ito, S. Okajima, K. Nakayama and R.J. Wylde, *Rev. Sci. Instrum.* **75**, 3508 (2004).
- [4] K. Kawahata, T. Akiyama, R. Pavlichenko, K. Tanaka, T. Tokuzawa, Y. Ito, S. Okajima, K. Nakayama and K. Wood, *Rev. Sci. Instrum.* **77**, 10F132 (2006).
- [5] V.S. Voitsenya, A.J. H. Donn , A.F. Bardamid, A.I. Belyaeva, V.L. Bereznyj, A.A. Galuza, Ch. Gil, V.G. Konovalov, M. Lipa, A. Malaquais, D.I. Naidenkova, V.I. Ryzhkov, B. Schunke, S.I. Solodovchenko and A.N. Topkov, *Rev. Sci. Instrum.* **76**, 083502 (2005).
- [6] H. Soltwich, *Plasma Phys. Control. Fusion*, **35**, 1777 (1993).
- [7] K. Kawahata, K. Tanaka, T. Tokuzawa, Y. Ito, A. Ejiri and S. Okajima, *Rev. Sci. Instrum.* **71**, 707 (1999).
- [8] J.P. Crenn, *Applied Optics* **21(24)**, 4533 (1982).
- [9] I. Benfatto, P. Bettini, M. Cavinato, A. De Lorenzi, J. Hourtoulle and E. Serra, *Fusion Engineering and Design* **75-79**, 235 (2005).
- [10] G. Braithwaite, N. Gottardi, G. Magyar, J. O’Rourke, and D. Veron *Rev. Sci. Instrum.* **60**, 2825 (1989).
- [11] T. Shikama *et al.*, *Nucl. Fusion* **43(7)**, 517 (2003).
- [12] V.S. Voitsenya, Private communications.